Michael Sean Chenoweth. Morphometric analysis of gypsum depressions using drone imagery at sinkhole flat, Eddy County, New Mexico, USA. *Journal of Cave and Karst Studies*, v. 88, no. 3, p. 100-108. DOI: 10.4311/2022ES0105

MORPHOMETRIC ANALYSIS OF GYPSUM DEPRESSIONS USING DRONE IMAGERY AT SINKHOLE FLAT, EDDY COUNTY, NEW MEXICO, USA

Michael Sean Chenoweth[C]

Abstract

Morphometric analysis is conducted on five karst depressions in Permian-age gypsum of southeast New Mexico. These depressions take on the form of classically shaped blind valleys and sinkholes. Blind valleys in this study are disappearing surface streams composed of multiple tributaries that connect to the main trunk channel leading to a cave entrance. A visible light (RGB) sensor mounted on a quadcopter is used to collect aerial imagery for karst depression mapping and analysis. Field measurements were taken for each depression for comparison with the drone imagery and its derivative layers such as digital elevation model (DEM) and slope. Drone flight elevations were set to 45 m above ground level (AGL) except for one site, which was 76 m AGL, resulting in a spatial resolution ranging from 0.78 to 2.37 cm. A total of 505 images were taken for all sites and mosaiced with photogrammetry software for geospatial analysis. The average field measured depth is 7.5 m and the average DEM measured depth is 5.48 m. DEM measured perimeter ranged from 77 to 675 m and volume ranged from 129 to 4,339 m^3. All DEM measured slopes were less than field measured slopes with the differences ranging from −1° to −39°. Drone orthomosaics and DEM-derived layers make it possible to visualize and quantify the complex morphology of the karst depressions that are not clearly discernible from the ground. Drone imagery can be used to rapidly map and assess gypsum depressions in arid areas.

INTRODUCTION

Gypsum and salt are the most soluble of common evaporite rocks. Evaporite karst features can form rapidly, within days, weeks, or years, whereas carbonate karst features take years, decades, or centuries to form. Water percolates over or through gypsum, causing the formation of sinkholes, disappearing streams, natural bridges, caves, and springs (Johnson, 1997).

Sinkholes are numerous in southeast New Mexico wherever beds of salt and gypsum lie near the surface and the ranchmen fence them to prevent cowboys from riding into them (Lobeck, 1939). Sinkholes and karst fissures formed in gypsum bedrock are common features in the lower Pecos Valley region of New Mexico and West Texas (Land, 2013). In the Delaware Basin region, hypergene karst occurrences are dominated by surficial geomorphic expression of heavy karren development on exposed gypsum surfaces and extensive solutional sinkhole development is often associated with well-developed, dendritic arroyo drainage networks (Stafford et al., 2018).

The Permian Basin of the American Southwest represents the most widespread and pronounced examples of gypsum and salt karst in the United States (Johnson, 1997). Permian evaporites in southeastern New Mexico include gypsum, anhydrite, and salt. Dissolution has produced hundreds of individual karst features including collapse sinks, karst valleys, blind valleys, karst plains, caves, and breccia pipes (Bachman, 1987).

A blind valley is a gorge that terminates abruptly at a point where the stream sinks (Gilli, 2015). Blind valleys have been documented by other researchers in southeastern New Mexico. Blind valleys commonly develop in the thick upper sulfate of the Tamarisk Member in the Nash Draw karst valley 30 km east of Carlsbad, New Mexico (Powers et al., 2006). Bachman (1987) suggests that in semiarid southeastern New Mexico, the term “blind arroyo” is a more descriptive name for “blind valleys.” Blind arroyos are small, deep flat-bottomed gullies with intermittent flow occurring after heavy rain. A steep bank marks the termination of the arroyo at a collapse sink or cave. Half blind arroyos back up headward in the arroyo during intense rainfall. Stafford et al. (2008) conducted field studies in the Castile Formation evaporite karst region of southeast New Mexico, measuring sinkhole length, width, and depth. Their findings were that sinkhole area and volume varied widely within the surveyed sites (see pages 37–38 for detailed morphometric measurements).

Numerous sinkhole studies using drones and LiDAR have been published effectively delineating and quantifying doline physical attributes (Silva et al., 2017; Kim et al., 2019; Mihevc and Mihevc, 2021). A literature gap exists in the use of visible light (RGB) drones and evaporite karst surface morphology. Fewer studies have used drones to map and measure sinkholes using visible light (RGB) sensors. Gijón-Yescas et al. (2021) compared drone-derived orthomosaics to Google Earth images of a large complex cenote in the Yucatan, Mexico. Drone imagery was able to obtain much finer measurement results compared with satellite-derived Google Earth imagery. Even for a large depression, such as cenotes in urban areas, drone imagery is superior to high-resolution satellite data.

Department of Chemistry & Geosciences, Jacksonville State University, Jacksonville, Alabama 36265
[C]Corresponding author: mchenoweth@jsu.edu.

STUDY AREA

The study area is situated in the northeastern Chihuahuan Desert Great Plains region (Medellín-Leal, 1982) about 16 km west of Brantly Lake State Park in Eddy County, New Mexico, USA (Fig. 1). The Pecos Valley forms the southern end of the Great Plains where the surface is almost flat with an average altitude of 750 m (Medellín-Leal, 1982). Hydrologically, the study area is located in the USGS Rio Grande Region. The karst features discussed in this paper are within the Long Draw–South Seven Rivers Hydrologic Unit (HUC12 130600110505). The study site can also be found on the USGS 7.5-min topographic quadrangle named Foster Ranch, NM (Latitude +32.5412°, Longitude −104.5857°).

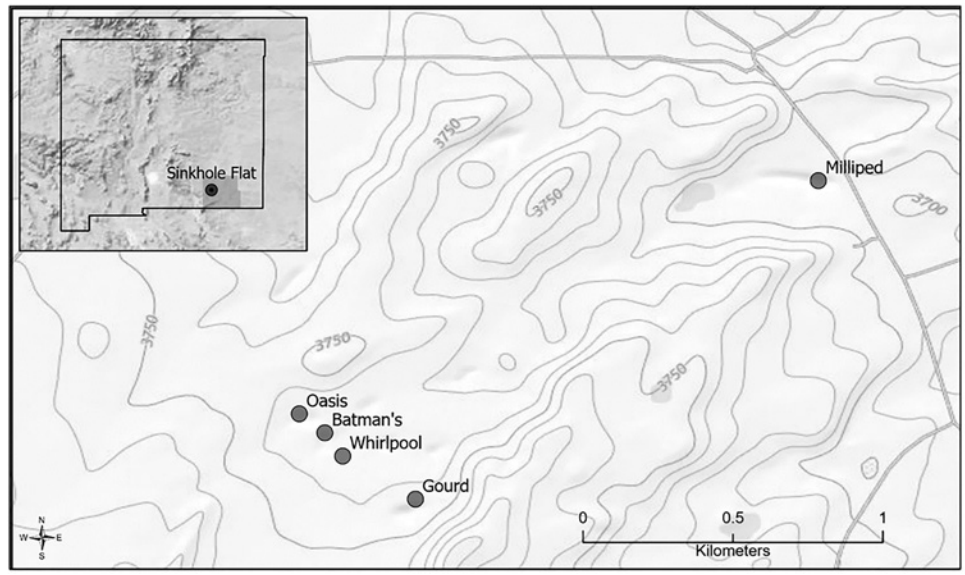


Figure 1. Location of karst depressions in this research paper at Sinkhole Flat in Eddy County, New Mexico, USA (USGS 7.5 topo Foster Ranch, NM).

Gypsum karst is best expressed where mean annual precipitation is low (Ford and Williams, 2007). Gypsum karst is fairly common in the semiarid to arid regions of the western United States (Johnson, 1997). The Köppen climate classification for Carlsbad, New Mexico, is cold desert (BWk). The average annual maximum temperature is 25.8 °C, and the average annual minimum temperature is 8.4 °C. The average annual total precipitation is 32.6 cm, with an average snow depth of 11.2 cm (WRCC, 2022). The Lower Sonoran life zone in the Pecos Valley is mainly composed of mesquite, black grama grass, *Optunia*, *Yucca*, *Larrea*, and *Acacia* (Beck and Hasse, 1969; Cokendolpher and Polyak, 1996).

Sinkhole Flat is located in the evaporite facies of the Grayburg Formation (Permian/Guadalupian Series/Artesia Group), which consists of sandstone, gypsum, anhydrite, dolomite, and red mudstone. The Artesia Group is the shelf or back reef facies of the Guadalupian Series including the Queen Formation overlying the Grayburg Formation (Tait et al., 1962). Gypsum is the dominant evaporitic rock at the surface where karst features including collapse sinks and karst valleys are prominent in the Artesia Group north of Carlsbad, New Mexico (Bachman, 1987). The gypsum caves of Sinkhole Flat form along and within surface drainage systems and probably migrate with the denudation of the region where the soluble Permian gypsum units crop out. These caves formed relatively fast and are probably short-lived (Cokendolpher and Polyak, 1996).

METHODS

Field measurements were taken for each depression for comparison with the drone imagery and its derivative layers such as the digital elevation model (DEM) and slope. Field measurements focused on the physical characteristics associated with the stream sink area. All depressions in this study have a cave associated with their deepest point. Slope and joint orientations were taken with an analog compass and clinometer. The magnetic declination for the compass was set to +6° East. The internal slopes of each karst depression were measured in the four cardinal directions (north, south, east, and west) at a height of approximately 1 m above the lowest point of the depression (Chenoweth, 1997). The depth of the karst depressions was measured from the bottom up. The top was defined as the elevation of the highest closed contour surrounding the depression. To determine this top edge accurately, careful field observations were made. Each contour line was identified and confirmed by walking the perimeter of the depression and using a GPS for elevation data. Length and width measurements were made with a standard field measuring tape after each karst depression's highest closed contour was determined through careful observation in the field. The length of each depression was defined as the longest straight line corresponding to the ephemeral surface stream entering the karst depression. The width was then measured as the longest line perpendicular to this length.

Each depression was surveyed using a small, unmanned aircraft system (sUAS) or drone. The DJI Phantom 4 Pro Version 2 is a quadcopter that comes with a visible light (RGB) camera, and it costs approximately $1,200. This drone was selected primarily for its mechanical shutter, which eliminates rolling shutter distortion when capturing still images during autonomous flights. The camera has a 2.54 cm (1 in.) CMOS sensor to record 20 megapixel still images. Image

size settings included a 3:2 aspect ratio with a width of 5,472 pixels and height of 3,648 pixels. Images and videos were stored on a high-speed Micro SD card (64GB, UHS-3) inserted into the drone fuselage.

Drone mission planning and automated drone flights were performed using Pix4D Capture software operating on an Apple iPad mini connected to the drone's remote control or ground control station (GCS). Image overlap was set to 70% forward and 60% side for all missions (Fig. 2). Flight elevations for each drone survey were set to a constant altitude of 45 m above ground level (AGL) from the initial takeoff point adjacent to each karst depression, except for Gourd BV, where the elevation was 76 m AGL (Table 1).

Drone2Map (ESRI version 2.3.2) is a photogrammetry software used to create orthomosaics and digital terrain models (DTMs) or digital elevation models (DEMs) from images taken by the drone over each karst depression. The software also generates 3D point clouds enabling volumetric measurements of features in a scene. The processing time for each drone survey dataset in Drone2Map averaged approximately 40 min using a high-performance desktop workstation. Orthomosaics and DEMs were exported from Drone2Map into ArcGIS Pro (ESRI version 2.9.1) for integrative geospatial analysis.

The drone-derived DEM was used in ArcGIS Pro to create contours, slope models, linear, area, and volumetric measurements. Perimeter, area, and volume (Table 4) were calculated using the upper closed depression contour associated with each karst depression (Figs. 4–6). Contours for the digital elevation models (DEMs) of each study site were generated, originating from the lowest point of the depression. The lowest point for each DEM was calculated using a raster tool in ArcGIS Pro called Highest or Lowest.

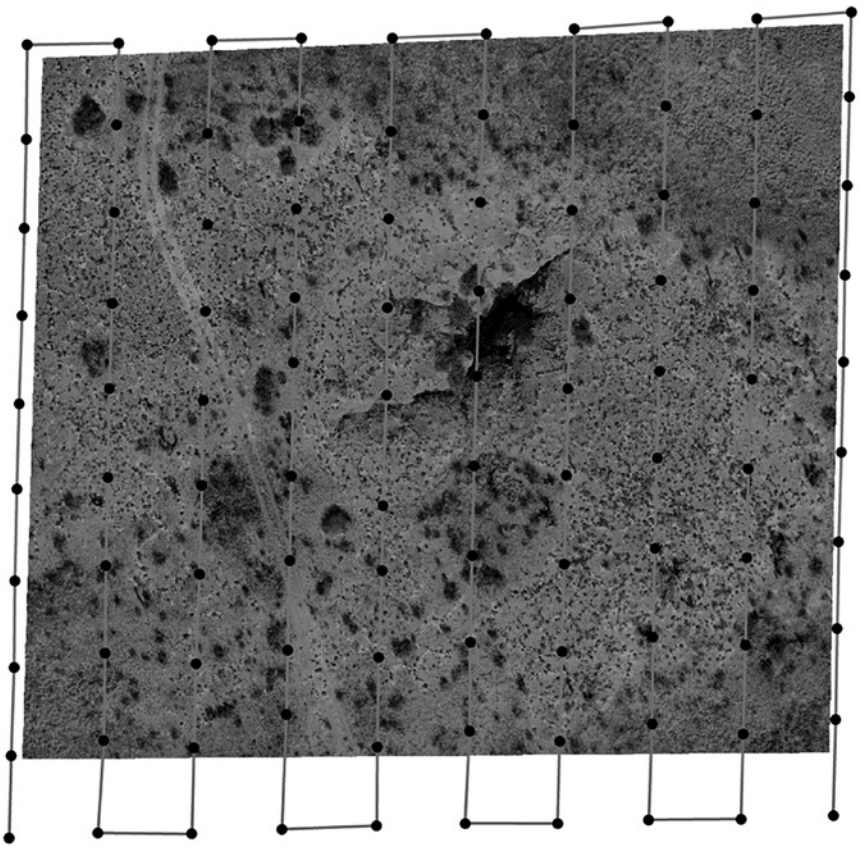


Figure 2. Drone flight lines for Whirlpool Sink. The dots show the location of each photograph taken (100 images total). Orthomosaic shown in the background is a clipped version of the original mosaic. Note dirt track on the left side of sinkhole.

Table 1. Drone autonomous flight attributes for each depression.

Site Name	# Photos	Flight Elev. (m)	Spatial Res. (cm)
Oasis	135	45	0.78
Batman's	57	45	0.78
Whirlpool	100	45	0.81
Gourd	25	76	2.37
Milliped	188	45	0.92

RESULTS

Field Investigation

The depressions in this study, except for Whirlpool sink, are blind valleys (BVs) with a cliff foot sink point at the downstream blind end. Well-developed rillenkaren, reminiscent of tropical karst, is present on various steeply sloped areas throughout the gypsum depressions. The names of these depressions come from round metal Bureau of Land Management (BLM) identification plaques bonded to the bedrock outside of each cave entrance (Oasis, Batman's, Whirlpool, Gourd, Milliped). The BLM has confirmed that the spelling of Milliped is correct.

Oasis blind valley (Fig. 3) has a cave with 7-m-high ceilings and a meandering serpentine passage typical of gypsum caves explored in this area. The major joint orientation is 50° (Table 2) and the depth is 7.62 m (Table 3). The field measured length is 105.46 m and the width is 77.72 m (Table 4). The field measured internal slopes are as follows: Slope north (Sn) 48°, Slope east (Se) 85°, Slope south (Ss) 40°, and Slope west (Sw) 30° (Table 5).

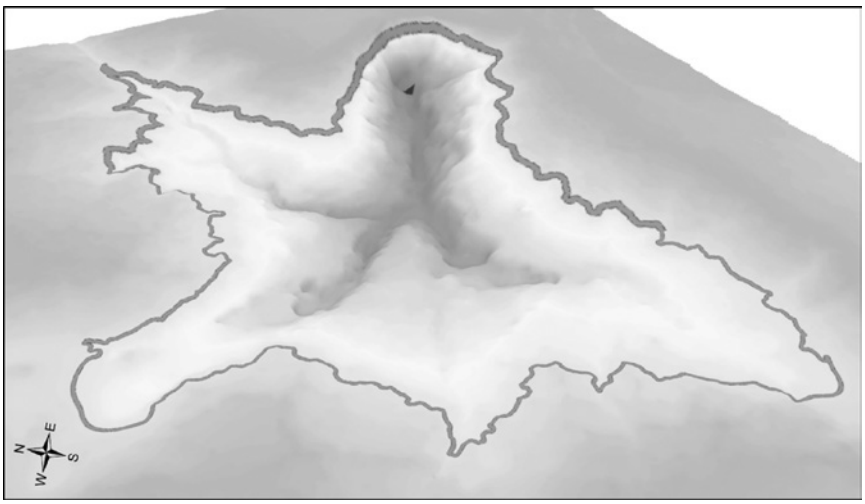


Figure 3. Oasis blind valley DEM 3D view (scale varies in this perspective). The solid line delineates the upper closed contour and the triangle is the lowest point in the DEM.

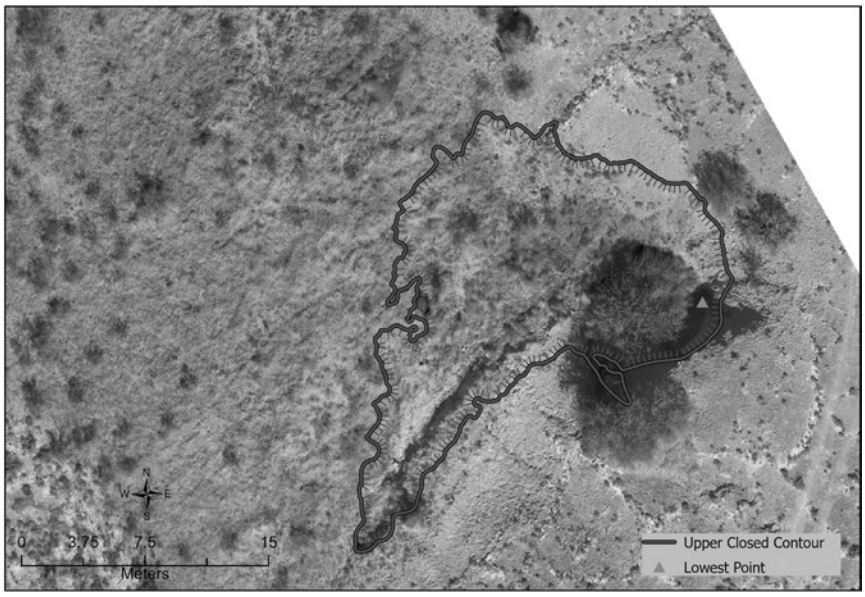


Figure 4. Batman's blind valley orthomosaic shows surface drainage entering from the NNE and SSW. Large mesquite tree adjacent to the lowest point.

Batman's cave (Fig. 4) is also a blind valley with a 1.7-m-high cave entrance facing north under a 3.5-m-high cliff (Table 3). Several surface streams converge on the depression and lead to the cave entrance. A large mesquite tree grows near the cave entrance in the base of the depression. There is a well-beaten path to the bottom where cattle take respite from the heat. The major joint orientation is 110° (Table 2) and the depth is 3.05 m (Table 3). The length is 16.46 m, and the width is 13.41 m (Table 4). Internal slopes are as follows: Sn 30°, Se 40°, Ss 90°, and Sw 42° (Table 5).

Whirlpool sink (Fig. 5) is deep, with few surface tributaries, and steep vertical walls. There is a cave entrance about 2 m high and 1 m wide in the southwest part of the sinkhole beneath a steep slope. Rillenkarren is particularly abundant, and a layer of red sandstone is exposed at the base. The major joint orientation is 30° (Table 2), with a minor joint orientation of 120°. The deepest section is at the cave entrance, measuring 9.14 m from the surface (Table 3). The length is 19.81 m and the width is 17.67 m (Table 4). Internal slopes are as follows: Sn 50°, Se 78°, Ss 72°, and Sw 80° (Table 5).

Gourd blind valley (Fig. 6) has a tight squeeze cave entrance about 45 cm high and 50 cm wide with a major joint orientation of 95° (Table 2) and a depth of 7.01 m (Table 3). Drainage flows into the depression from the east. The length is 19.81 m and the width is 13.41 m (Table 4). Internal slopes are as follows: Sn 40°, Se 20°, Ss 40°, and Sw 50° (Table 5).

Milliped blind valley (Fig. 7) or Barbed Wire Cave (Cokendolpher and Polyak, 1996) is the largest blind valley by volume (Table 4) in this study and is located northeast of the main cluster of depressions (Fig. 1). This elongated blind valley is oriented east–west with a cave entrance on the topographically lower eastern side. The major joint orientation is 60° (Table 2) and the deepest point is 10.67 m (Table 3). Internal slopes adjacent to the cave entrance are as follows: Sn 75°, Se 62°, Ss 90°, and Sw 20° (Table 5). The length and width of this depression were not measured in the field due to the large size and safety considerations near the precipice edges. Primary drainage flows into the depression from the west with several first order surface tributaries entering the trunk channel. There are three other prominent geomorphic features associated with this depression: a karst window, a small sinkhole, and a stream meander. The karst window is located about 15 m east and upslope from the cave entrance and the vadose stream passage has a joint orientation of 160° (Table 2). The small sinkhole (Fig. 7) is in the main trunk channel about 96 m west of the cave entrance. It is about 70 cm deep, with the same joint orientation as the karst window, crossing the wall of the blind valley. The stream meander is located about 22 m west of the cave entrance.

Geospatial Investigation

The number of survey photographs taken for each depression ranged from 57 to 188, with a total of 505 images (Table 1). The spatial resolution or pixel size is directly related to flight elevation and ranged from 0.78 to 2.37 cm. Gourd

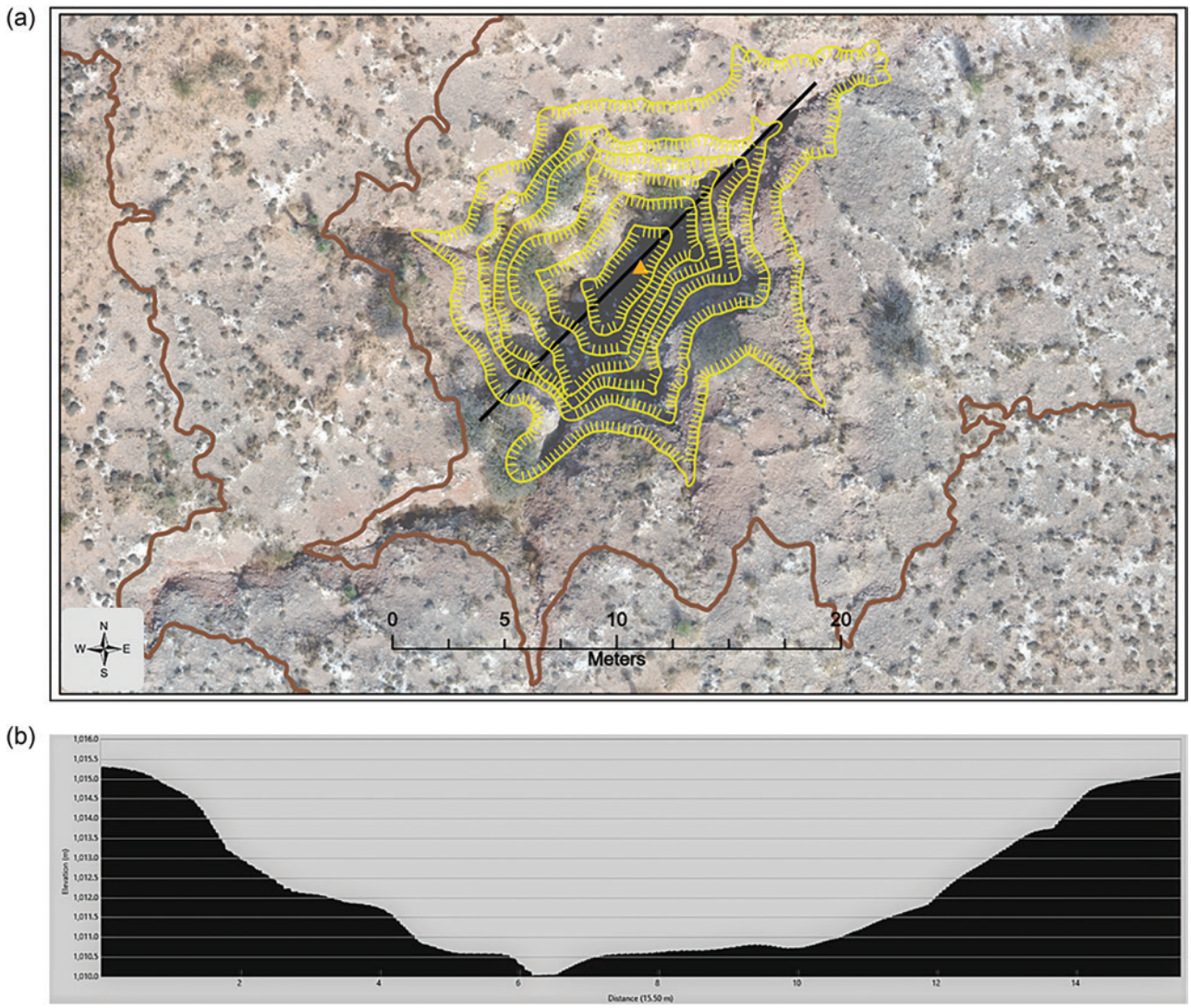


Figure 5. Drone-generated orthomosaic of Whirlpool sink. (A) Yellow-hatched contours demarcate the sinkhole, the orange triangle represents the lowest point, and the brown lines are open contours leading away from the depression. Contours are at 1-m intervals. (B) Elevation profile represented by the black line in the orthomosaic. Drone-derived elevations are relative to the takeoff point and depend on the accuracy of the GNSS at the time of flight.

BV flight elevation was set at a higher flight elevation of 76 m instead of 45 m (Fig. 2) so that the mission could be completed on one battery from the location of the GCS. The flight elevation increase resulted in 2.37 cm spatial resolution instead of sub-one-centimeter spatial resolution for all other depression flights. The vertical accuracy ranged from 2.34 to 7.11 cm.

Depth measured from the drone-derived DEM was obtained from the lowest calculated point to the upper closed contour. DEM depth ranged from 1.54 to 7.46 m, with an average of 5.48 m (Table 3). DEM measured length ranged from 27.9 m (Whirlpool) to 211.8 m (Milliped) with an average of 92.3 m, while the width varied from 21.2 m (Whirlpool) to 83.8 m (Oasis), averaging 48.1 m (Table 4).

The DEM measured perimeters ranged from 77.1 m at Whirlpool sink to 675.4 m at Milliped BV. The average for all five features is 304.3 m (Table 4). The DEM surface area ranged from 179.6 m^2 at Whirlpool sink to 2,601.8 m^2 at Oasis BV, with an average of 1,422.76 m^2 (Table 4). The average depression volume measured from the DEM is 2,152.6 m^3, where Batman's BV is 129.2 m^3 and Milliped BV is 4,339.4 m^3 (Table 4).

Table 6 summarizes all the slope values calculated from the DEM below the upper closed contour for each depression. The GIS software calculates the slope values for all pixels within the depression. The minimum slope value for all depressions is 0.0° except for Whirlpool sink at 0.1°. Gourd BV has the lowest maximum slope value at 60° and Milliped BV has the steepest maximum aggregated slope values of 78.4°. Gourd BV has the lowest mean value of 12.3° while Whirlpool sink has the highest mean slope value of 38.2°. The standard deviation was lowest for Gourd BV (9.7) and

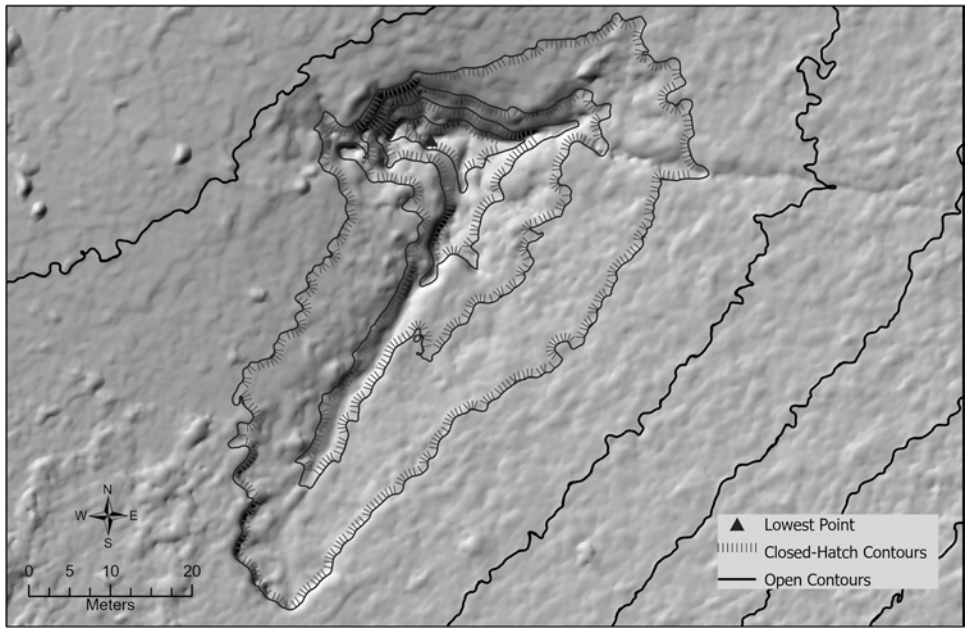


Figure 6. Hillshade model and 1-m contours of Gourd blind valley generated from drone DEM.

Table 2. Joint orientations associated with each karst depression measured in the field.

Site Name	Joint Orientations
Oasis	50°
Batman's	110°
Whirlpool	30°, 120°
Gourd	95°
Milliped	60°, 160°

Table 3. Comparison of field measured depth to DEM depth.

Site Name	Field Depth (m)	DEM Depth (m)	Difference
Oasis	7.62	7.46	−0.16
Batman's	3.05	1.54	−1.51
Whirlpool	9.14	6.71	−2.43
Gourd	7.01	4.32	−2.69
Milliped	10.67	7.37	−3.30
$\bar{x}$	7.50	5.48	−2.02

the highest was for Whirlpool sink (15.6).

DISCUSSION

Many minor karst features in gypsum in southeast New Mexico remain to be catalogued and described in detail (Bachman, 1987). This paper seeks to fill this literature gap with detailed field- and drone-derived DEM measurements of gypsum karst depressions at Sinkhole Flat. There are fourteen large karst depressions in the vicinity of Sinkhole Flat, several of which are not on BLM land. This research focused on five depressions that were difficult to measure in the field due to size, complexity, and safety. The edges of some depressions are steep, fragile, and unstable, making it dangerous to measure the landforms accurately in the field.

LiDAR drones are expensive and exceed the budget of most academic departments' discretionary funds. Also, there are often additional software and hardware purchases, such as proprietary image processing software and RTK GPS, necessary to make the LiDAR data accurate and functional. Sinkholes and other surface geomorphic features can be accurately mapped and characterized using inexpensive visible light (RGB) drones. High-spatial resolution drone DEMs allow for detailed delineation of morphologically complex karst depressions using quantitative methods based on the topography.

Table 4. Field measured length and width and DEM measured length, width, perimeter, area, and volume.

	Field Measured		DEM Measured				
Site Name	Length (m)	Width (m)	Length (m)	Width (m)	Perimeter (m)	Area (m^2)	Vol. (m^3)
Oasis	105.46	77.72	103.60	83.80	388.90	2601.80	4130.50
Batman's	16.46	13.41	31.70	22.70	126.60	298.30	129.20
Whirlpool	19.81	17.67	27.90	21.20	77.10	179.60	340.00
Gourd	19.81	13.41	86.50	45.10	253.60	2074.80	1823.90
Milliped	—	—	211.8	67.70	675.40	1959.30	4339.40

Table 5. **Comparison of field measured cardinal slopes* versus DEM measurements.**

	Field Measurements				DEM Measurements				Differences			
Site Name	**Sn°**	**Se°**	**Ss°**	**Sw°**	**Sn°**	**Se°**	**Ss°**	**Sw°**	**Sn°**	**Se°**	**Ss°**	**Sw°**
Oasis	48	85	40	30	45	67	38	28	−3	−18	−2	−2
Batman's	30	40	90	42	27	39	53	15	−3	−1	−37	−27
Whirlpool	50	78	72	80	49	55	62	54	−1	−23	−10	−26
Gourd	40	20	40	50	33	18	37	48	−7	−2	−3	−2
Milliped	75	62	90	20	68	61	51	18	−7	−1	−39	−2

*Slope north (Sn), Slope east (Se), Slope south (Ss), Slope west (Sw).

Table 6. Summary statistics for all DEM slope values, in degrees, below the upper closed contour.

Site Name	Min	Max	Mean	Std. Dev.
Oasis	0.0	77.4	19.2	13.3
Batman's	0.0	73.3	13.8	10.6
Whirlpool	0.1	79.1	38.2	15.6
Gourd	0.0	60.0	12.3	9.7
Milliped	0.0	78.4	36.1	15.2

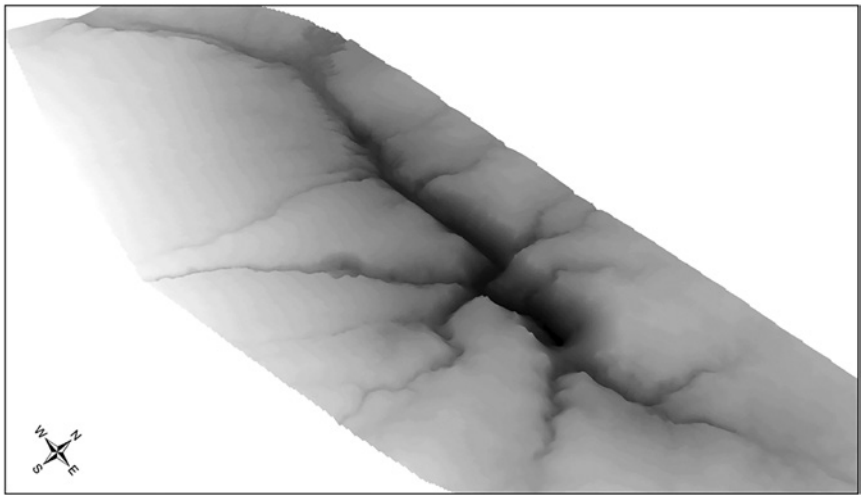


Figure 7. 3D elevation model of Milliped blind valley and tributaries (scale varies in this perspective).

One of the disadvantages of using a visible light sensor is the obstruction of geomorphic details by vegetation, even in arid regions. While conducting field work, some of the depressions had large clusters of wind-blown tumbleweed accumulated in narrow or low places including cave entrances. Contour lines generated from the DEM in a GIS are affected by heaps of dead vegetation, taller living vegetation, and the brittle, crumbly nature of gypsum near depression edges.

The mean field measured depression depth was 7.5 m while the mean DEM measured depth was 5.48 m (Table 3). All DEM depths were less than the actual field measured depths, ranging from −0.16 m for Oasis BV to −3.3 m for Milliped BV. Since there are significant differences between the field measured depths and drone measured depths, perhaps a double grid pattern could be flown for additional images to potentially capture more angles to map the depression depth more accurately.

Oasis BV has the largest surface area of 2,601.8 m^2 (Table 4), but Milliped BV has the largest volume of 4,339.4 m^3 (Table 6). This may be related to slope values where the Oasis BV average slope is 19.2° m and Milliped BV average slope is 36.1° m (Table 6). Perimeter is the continuous line forming the boundary of a closed geometric figure. Oasis BV has the second longest perimeter of 388.9 m compared to Milliped BV, which has the longest perimeter of 675.4 m.

Batman's BV has unique hydrogeomorphic conditions that allow a large mesquite tree (Fig. 4) to grow in its base adjacent to the cave entrance. This large tree conceals the morphology of the blind valley so that when the drone-generated DEM is used to measure the morphometric characteristics, it appears shallower and with gentler slopes (Tables 3, 5, and 6). Also, this blind valley has the lowest volume of only 129.2 m^3 because of the presence of a tree in its deepest section. Batman's BV is also the shallowest depression with a field measured depth of 3.05 m compared to 1.54 m measured from the DEM (Table 3).

Whirlpool sink was the only true sinkhole in this study. It is the most compact depression with the lowest surface area of 179.6 m^2 and shortest perimeter of 77.1 m (Table 4). It has the 2nd deepest field measured depth of 9.14 m, but its DEM measured depth ranked 3rd deepest (Table 3). This small anomaly is probably due to topographic shadowing associated with its steep slopes affecting accurate DEM generation and a layer of tumbleweed at the bottom. DEM measured slopes for Whirlpool sink are the steepest in the study, ranging from 0.1° to 79.1°, with an average of 38.2° (Table 6).

Gourd BV flight elevation was set at a higher flight elevation of 76 m instead of 45 m so that the mission could be completed on one battery from the location of the GCS. The flight elevation increase resulted in 2.37 cm (Table 1) spatial resolution instead of sub-one-centimeter spatial resolution for all other depression flights. In the field, it was noted that the surface drainage originates from the east. Examination of the DEM illustrates the elongated NNE–SSW shape of the depression and the broad, shallow surface drainage originating from the SSW (Fig. 6). Surface drainage originating from the east aligns with the cave entrance joint orientation of 95° (Table 2) and is readily apparent in the field.

Milliped BV is oriented east–west and is long, narrow, and deep with more than a dozen first-order tributaries (Fig. 7). It has the deepest field measured depth of 10.67 m, but its DEM measured lowest point is 7.37 m (Table 3). The east–west orientation of this depression created shadows on the south slopes (northern aspect) during the drone flight, concealing details of depth and slope. Field measured slopes reveal the shadowing effect when compared to the DEM slopes. The field measured southern slope adjacent to the cave entrance is 90° and the equivalent location on the DEM is 51°, which is a −39° difference (Table 5). Milliped's DEM measured length is 211.8 m, which is more than twice the length of Oasis. Milliped BV also has the longest perimeter of 675.4 m and the greatest volume of 4,339.4 m^3 (Table 4).

One of the limitations of this study was the lack of documentation of the exact locations for field length and width measurements. Oasis BV field versus DEM measurements (Table 4) were relatively similar, followed by Whirlpool sink. Both depressions are deep with easily recognized boundaries in the field. However, the remaining depressions' dimensions and morphology were difficult to determine in the field due to the subtle nature of surface tributaries for Batman's and Gourd blind valleys (Figs. 4 and 6). In the case of Milliped BV, the numerous deeply incised tributaries (Fig. 7) made it challenging to demarcate the outline of this depression in the field. Drone images were not processed in the field while camping at Sinkhole Flat due to limited resources; each drone flight required about 1 h of computer processing time, and the vehicle was only used for charging drone batteries via an inverter.

CONCULSIONS

Inexpensive visible light (RGB) drone imagery can be used to create relatively accurate maps for karst depression and geomorphometric analysis in sparsely vegetated arid areas. Surface area can be measured accurately, but because depth is obscured by shadows and vegetation, drone measured depths can vary by several meters.

Drone orthomosaics and DEM-derived layers make it possible to visualize and quantify the complex morphology of the karst depressions that cannot easily be seen from the ground. Drone imagery can be used to rapidly map and assess gypsum depressions in arid areas. The use of an affordable RGB drone to map surface features is possible in arid areas, open fields, sparsely vegetated outcrops, or low-density urban areas.

Terrain shadows and low sun angles obscure the true depth and slope values of drone-generated DEM's and slope models. A double grid pattern (flight lines perpendicular to each other) flown by the drone will increase the number of images collected from different angles to increase DEM accuracy and thereby improve the accuracy of derivative layers such as contouring and slope values. Drone flights should occur between the hours of 11:00 am and 1:00 pm to reduce topographic shadowing of karst depressions and to improve the accuracy of the DEM.

REFERENCES

Bachman, G. O., 1987, *Karst in Evaporites in Southeastern New Mexico*: Albuquerque, New Mexico, Sandia National Labs., https://www.osti.gov/biblio/5947512

Beck, W. A and Hasse, Y. D., 1969, *Historical Atlas of New Mexico*: Norman, Oklahoma, University of Oklahoma Press, 62 p.

Chenoweth, M. S., 1997, The spatial distribution and morphometric analysis of dolines, Buffalo National River, Newton County, Arkansas [MA thesis]: Fayetteville, University of Arkansas, 94 p., https://www.proquest.com/docview/304338686?pq-origsite=gscholar&fromopenview=true.

Cokendolpher, J. C and Polyak, V. J., 1996, Biology of the caves at Sinkhole Flat, Eddy County, New Mexico: Journal of Caves and Karst Studies, v. 58, no. 3, p. 181–192. https://caves.org/pub/journal/PDF/V58/v58n3-Cokendolpher.htm

Ford, D. C and Williams, P., 2007, *Karst Hydrogeology and Geomorphology*: Chichester, England, John Wiley, 562 p., https://doi.org/10.1002/9781118684986.

Gijón-Yescas, N. G., Aguilar-Duarte, Y. G., Frausto-Martínez, O., and Bautista-Zuñiga, F., 2021, Anatomy of a Cenote with use of Dron: Tropical and Subtropical Agroecosystems, v. 24, no. 30, p. 1–14, https://www.revista.ccba.uady.mx/ojs/index.php/TSA/article/view/3634

Gilli, É., 2015, *Karstology: Karsts, Caves and Springs: Elements of Fundamental and Applied Karstology*: Boca Raton, Florida, CRC Press, 256 p.

Johnson, K. S., 1997, Evaporite karst in the United States: Carbonates and Evaporites, v. 12, no. 1, p. 2–14, https://doi.org/10.1007/BF03175797

Kim, Y. J., Nam, B. H., and Youn, H., 2019, Sinkhole detection and characterization using LiDAR-derived DEM with logistic regression: Remote Sensing, v. 11, no. 13, p. 1592, https://doi.org/10.3390/rs11131592

Land, L., 2013, Geophysical records of anthropogenic sinkhole formation in the Delaware Basin region, southeast New Mexico and west Texas, USA: Carbonates and Evaporites, v. 28, no. 1–2, p. 183–190, https://doi.org/10.1007/s13146-013-0126-9

Lobeck, A. K., 1939, *Geomorphology, An Introduction to the Study of Landscapes*: New York, McGraw-Hill Book Company, 731 p.

Medellín-Leal, F., 1982, The Chihuahuan desert, *in* Bender, G. L., ed., *Reference Handbook on the Deserts of North America*: Westport, Connecticut, Greenwood Press, 594 p.

Mihevc, A and Mihevc, R., 2021, Morphological characteristics and distribution of dolines in Slovenia, a study of a LiDAR-based doline map of Slovenia: Acta Carsologica, v. 50, no. 1, p. 11–36, https://doi.org/10.3986/ac.v50i1.9462

Powers, D. W., Beauheim, R. L., Holt, R. M., Hughes, D. L., and Land, L., 2006, Evaporite karst features and processes at Nash Draw, Eddy County, New Mexico, *in* New Mexico Geological Society Fall Field Conference Guidebook, Volume 57: Socorro, New Mexico, New Mexico Geological Society, p. 253–266.

Silva, O. L., Bezerra, F. H., Maia, R. P., and Cazarin, C. L., 2017, Karst landforms revealed at various scales using LiDAR and UAV in semi-arid Brazil: Consideration on karstification processes and methodological constraints: Geomorphology, v. 295, p. 611–630, https://doi.org/10.1016/j.geomorph.2017.07.025

Stafford, K. W., Rosales-Lagarde, L., and Boston, P. J., 2008, Castile evaporite karst potential map of the Gypsum Plain: Eddy County, New Mexico and Culberson County, Texas: a GIS Methodological Comparison: Journal of Cave and Karst Studies, v. 70, no. 1, p. 35–46, https://caves.org/pub/journal/PDF/v70/cave-70-01-35.pdf

Stafford, K. W., Ehrhart, J. T., Majzoub, A. F., Shields, J. M., and Brown, W. A., 2018, Unconfined hypogene evaporite karst: West Texas and southeastern New Mexico, USA: International Journal of Speleology, v. 47, no. 3, p. 293–305, https://doi.org/10.5038/1827-806X.47.3.2166

Tait, D. B., Ahlen, J. L., Gordon, A., Scott, G. L., Motts, W. S., and Spitler, M. E., 1962, Artesia group of New Mexico and West Texas: AAPG Bulletin, v. 46, no. 4, p. 504–517, https://doi.org/10.1306/BC74383B-16BE-11D7-8645000102C1865D

WRCC, 2022, Desert Research Institute (DRI) Western Regional Climate Center, wrcc.dri.edu: https://wrcc.dri.edu/cgi-bin/cliMAIN.pl?nm1469